

Combined oncolytic adenovirus carrying MnSOD and mK5 genes both regulated by survivin promoter has a synergistic inhibitory effect on gastric cancer

Shan-Shan LIU¹, Jin-Qing HU², Jin-Fa GU², Ai-Min NI², Wen-Hao TANG^{3*}, Xin-Yuan LIU^{2*}

¹Laboratory of Cell Biology, Xin-yuan Institute of Medicine and Biotechnology, College of Life Science, Zhejiang Sci-Tech University, Hangzhou, China; ²State Key Laboratory of Cell Biology, Center for Excellence in Molecular Cell Science, Chinese Academy of Sciences, Shanghai, China; ³Department of General Surgery, Huadong Hospital, Fudan University, Shanghai, China

*Correspondence: wenhaotang1969@aliyun.com; xyliu@sibcb.ac.cn

Received May 8, 2021 / Accepted August 3, 2021

Gastric cancer (GC) is one of the major causes of cancer-related mortality. The use of oncolytic virus for cancer gene-virotherapy is a new approach for the treatment of human cancers. In this study, a novel Survivin promoter-driven recombinant oncolytic adenovirus carrying mK5 or MnSOD gene was constructed, which was modified after deletion of the E1B gene. Human plasminogen Kringle 5 mutant (mK5) and manganese superoxide dismutase (MnSOD) are both potential tumor suppressor genes. By constructing Ad-Surp-mK5 and Ad-Surp-MnSOD oncolytic adenoviruses, we hypothesized that the combination of the two viruses would enhance the therapeutic efficacy of GC as compared to the one virus alone. The results of the *in vitro* experiments revealed that the combination of adenovirus carrying mK5 and MnSOD gene exhibited stronger cytotoxicity to GC cell lines as compared to the virus alone. Additionally, the virus could selectively kill cancer cells and human somatic cells. Cell staining, flow cytometry, and western blot analysis showed that the combination of two adenoviruses containing therapeutic genes could promote the apoptosis of cancer cells. *In vivo* experiments further verified that Ad-Surp-mK5 in combination with Ad-Surp-MnSOD exhibited a significant inhibitory effect on the growth of GC tumor xenograft as compared to the virus alone, and no significant difference was observed in the bodyweight of treatment and the normal mice. In conclusion, the combination of our two newly constructed recombinant oncolytic adenoviruses containing mK5 or MnSOD therapeutic genes could significantly inhibit gastric cancer growth by inducing apoptosis, suggestive of its potential for GC therapy.

Key words: gastric cancer, mK5, MnSOD, survivin, adenovirus

Gastric cancer (GC) is the fifth most prevalent cancer worldwide and the third leading cause of cancer-related mortality [1]. GC is one of the most common malignant tumors of the digestive system. At present, surgery is considered the only radical cure. The 5-year survival rate of early gastric cancer may reach 95%, but due to late diagnosis, most of the patients are diagnosed at advanced stages [2]. Despite advances in surgical techniques, radiotherapy, chemotherapy, and neoadjuvant therapy [3], GC still remains a serious global health burden [4]. Many cancers can be cured by surgery, yet most of the world's population does not have access to safe, affordable, and timely cancer surgery [5].

Worldwide interest in oncolytic viruses (OVs), a powerful new oncology drug, has increased remarkably with the approval of the first OV (Talimogene Laherparepvec) by the US Food and Drug Administration [6]. However, extensive

research showed that oncolytic virus therapy is limited in the treatment of solid tumors. We used a novel strategy called cancer-targeted gene-virotherapy (CTGVT) that combined the advantages of gene therapy and oncolytic virus therapy to produce a stronger anti-tumor effect than either gene or oncolytic virus therapy alone [7]. For example, ONYX-015 is oncolytic adenovirus (Ad) with the deletion of its viral protein E1B-55kDa gene. Due to the inability of the mutated protein to degrade P53, the selectivity of tumor replication is enhanced. The early gene E1B gene encoded by Ads mainly contains two kinds of polypeptides E1B-19 kDa and E1B-55 kDa. E1B-19 kDa is homologous of Bcl-2, which can prevent E1A-induced apoptosis by interfering with Bak, Bax interaction. By E1B-19 kDa protein-induced inhibition of FAS mediated apoptosis and inhibition of apoptosis of cancer cells through other apoptotic pathways, Ad

knockout E1B-19 kDa after virus replication in restricted in normal cells and cancer cells are not suppressed [8]. In the host, the E1B-55 kDa protein binds to P53, which consequently leads to the inhibition of viral replication. Therefore, OV-knockout E1B-55 kDa can't replicate in the normal cells, but the virus replicates normally in tumor cells lacking P53 function and causes tumor cells dissolve. However, the oncolytic adenovirus produced simply by deleting viral genes is not selective enough to prevent unnecessary tissue damage. Recently, tumor-specific promoters have become the most popular tool for controlling the oncolytic adenoviruses that strictly target cancer cells [9]. *Survivin*, a member of the apoptosis-inhibiting protein family, is overexpressed in several types of cancers but is not expressed in differentiated normal tissues [10]. The results suggest that the *Survivin* promoter is a specific promoter for a variety of cancers and may play a role in cancer gene therapy and that the *Survivin* promoter is more tumor-specific than the CMV promoter *in vivo* [11].

The anti-angiogenic protein K5 (human plasminogen Kringle 5) forms the *mK5* mutation by mutation of 71 leucine residues to arginine [12]. Studies have shown that *mK5* and K5 can considerably inhibit the proliferation of human umbilical vein endothelial cells (HUVECs) and induce the apoptosis of vascular endothelial cells *in vivo* and *in vitro*. Additionally, *mK5* has a stronger effect on the induction of HUVECs apoptosis [13]. Previous studies have shown that OV-mediated *mK5* can inhibit the growth of colorectal cancer [14] and prostate cancer [15]. Cancer often involves changes in the growth and proliferation of cells. DNA damage and excessive production of reactive oxygen species (ROS) have also been reported to be responsible for the development of cancer [16]. Antioxidant protein-containing manganese oxide dismutase (*MnSOD*) is one of the key enzymes for the scavenging of mitochondrial ROS [17], and is also a tumor suppressor protein [18]. Significant growth inhibition was observed in human esophageal squamous [19], PC-3 human prostate cancer [20, 21], MeWo melanoma [22], osteosarcoma [23], ovarian cancer [24, 25], MCF-7 breast cancer [26], colorectal cancer [27, 28], hepatocellular carcinoma [29], and pancreatic cancer cell lines [30]. Overexpression of *mK5* and *MnSOD* cDNA by plasmid transfection or adenovirus transduction in various types of cancer triggers growth inhibition *in vivo* and *in vitro*.

In this study, the *Survivin* promoter was used to regulate the expression of oncolytic adenovirus E1A. The tumor-targeting gene viruses Ad-Surp-*mK5* and Ad-Surp-*MnSOD* were constructed for the first time, carrying therapeutic genes *mK5* and *MnSOD*, respectively. Moreover, the combined application of two recombinant oncolytic adenoviruses in gastric cancer was studied for the first time. Under both *in vivo* and *in vitro* conditions, the combination of Ad-Surp-*mK5* and Ad-Surp-*MnSOD* was more effective in the inhibition of tumor growth than Ad-Surp-*mK5* or Ad-Surp-*MnSOD* alone. The combination of two recombinant adeno-

viruses promoted the apoptosis of tumor cells and exhibited no toxic effects on the normal human somatic cells.

Materials and methods

Cells and culture. The human gastric cancer cell lines (HGC-27, NCI-87, AGS), human embryonic kidney cell line (HEK 293), human normal lung epithelial cell (Beas-2B), human liver cell (QSG-7701), human colon epithelial cell (NCM-460) was purchased from Shanghai Cell Library, Chinese Academy of Sciences (Shanghai, China). The AGS cells were cultured in RPMI-1640 medium, and other cell lines were cultured in DMEM complete medium. The media was supplemented with 10% fetal bovine serum (Gibco BRL, Grand Island, NY, USA), and all cell lines were incubated in humidified air at 37 °C containing 5% CO₂.

Molecular construction and identification. A deasy system was used to recombine adenovirus in our laboratory. In this study, the vector of Ad5 virus, shuttle plasmid pShuttle, pCA13, and pCA13-*survivin* were used. The oncolytic adenovirus plasmid pShuttle-E1A-ΔE1B with E1B (19kDa, 55kDa) gene deleted by site-directed mutation was previously obtained and preserved, and the *mK5* and *MnSOD* genes were amplified from pXYA05-*mK5* and pXYA05-*MnSOD* respectively by reverse transcription-polymerase chain reaction (PCR). The target gene was cloned into pCA13 (by HindIII/XhoI double digestion) in a seamless cloning way to obtain pCA13-gene. The pCA13-*Survivin*, pCA13-*mK5*, and pCA13-*MnSOD* were amplified by PCR. The expression box containing the target gene was seamlessly cloned into the corresponding position of the modified shuttle plasmid pShuttle-E1A-ΔE1B to construct pShuttle-Surp (XhoI)-E1A-ΔE1B-transgene (BglII). All plasmids were verified by restriction enzyme digestion, PCR, and DNA sequence. HEK 293 cells were transfected with the Effectene® Transfection Reagent Transfection kit. To amplify the recombinant adenovirus, PCR was performed and the PCR primer sequences and seamless clone primer sequences used in the study are listed in Table 1.

Western blot analysis. When the multiplicity of infection (MOI) of the recombinant oncolytic adenovirus was 5, GC cells were infected, and the cell lysates were treated and collected after 48 h of incubation. Bradford method was used to detect protein concentration. The samples were run on the 10% polyacrylamide gel electrophoresis, and the proteins were transferred to the polyvinylidene difluoride (PVDF) membrane, which was subjected to blocking with 5% skimmed milk powder at room temperature for 30 min. This was followed by the incubation of the membranes with primary antibodies at 4 °C for 3 h. The primary antibodies used in the study were Caspase-3 (Cat #sc-56053; 1:10000), Caspase-9 (Cat #sc-56073; 1:10000), Cleaved-PARP (Cat #sc-56196; 1:10000), all purchased from Santa Cruz Biotechnology, CA, USA; Cleaved-caspase 9 (Cat #9509T; 1:10000), Caspase-8 (Cat #4927T; 1:1000), Cleaved caspase-8

Table 1. Sequences of primers.

Primers	Sequences
survivin	Forward: 5'-ATGGCCCTGTCTTCAGC-3' Reverse: 5'-TCACTCCTTCCTTCTCAGCC-3'
<i>mK5</i>	Forward: 5'-AATTCCTGGCATTATGCCC-3' Reverse: 5'-TCGATGCTAGACGATCCAGA-3'
<i>MnSOD</i>	Forward: 5'-ATGAAGCACAGCCTCCCCGA-3' Reverse: 5'-TTACTTTTTGCAAGCCATGT-3'
E1B 55kDa	Forward: 5'-CAAAGGTGGCACTTAGGC-3' Reverse: 5'-AGGAACAGCGGGTCAGTA-3'
E1B 19kDa	Forward: 5'-TACATCTGACCTCATGGAGG-3' Reverse: 5'-CTTGATGACCTTCTCTTGA-3'
CMV-Transgene-SV40 Ploy A	Forward: 5'-AATTCCTGGCATTATGCCC-3' Reverse: 5'-TCGATGCTAGACGATCCAGA-3'
Survivin fusion cloning	Forward: 5'-TGGTACCGCGCCGCTCGAGAATTCCTGGCATTATGCCC-3' Reverse: 5'-CTTCAAAGAACGCGCTCGAGTCGATGCTAGACGATAAGA-3'
<i>mK5</i> fusion cloning	Forward: 5'-AGTCTTCGAGTCGACAAGCTTAATTCCTGGCATTATGCCC-3' Reverse: 5'-TCGATGCTAGACGATCCAGAGTCAGCCAATAAAAAGGCC-3'
<i>MnSOD</i> fusion cloning	Forward: 5'-AGTCTTCGAGTCGACAAGCTTATGAAGCACAGCCTCCCCGA-3' Reverse: 5'-TTACTTTTTGCAAGCCATGTGTCAGCCAATAAAAAGGCC-3'

Abbreviations: MnSOD-manganese superoxide dismutase; mK5-mutated K5 (human plasminogen Kringle 5)

(Cat #8592T; 1:1000), Cleaved-caspase 3 (Cat #9664T; 1:10000), Bcl-2 (Cat #15071T; 1:1000), Bax (Cat #2772T; 1:1000), SOD2 (Cat #13141T; 1:1000) all purchased from Cell Signaling Technology, Beverly, USA; β -actin (Cat #AC028; 1:100000) purchased from ABclonal Technology, Shanghai, China; *mK5* (1:1000) purchased from HUABio, Hangzhou, China. This was followed by incubation with the corresponding secondary antibodies for 1.5 h and finally, the membranes were scanned for the protein of interest.

Cell counting kit-8 assays. The cells were cultured in 96-well plates at a density of 3,000 cells/well for 6 h. To each well, 10 μ l of the recombinant adenovirus after treatment (different MOI gradient). Afterward, a CCK-8 detection kit (Beyotime, Shanghai, China) was used to detect cell vitality. The cells were continuously cultured at 37°C for 4 h, and the absorbance was measured at 450 nm by enzyme-linked immunosorbent assay.

Flow cytometry analysis. The GC cells were cultured in 6-well plates and treated with recombinant oncolytic adenovirus for 48 h (MOI=5). After different treatments, the cells were subjected to treatment with trypsin and collected. Around 1×10^5 cells were resuspended into a 500 μ l binding buffer. The analysis was repeated three times according to the manufacturer's instructions of the Annexin V-FITC/PI kit (BD ISRI Corp, Franklin Lakes, USA).

EdU cell proliferation kit. The GC cells cultured in 24-well plates were treated with various recombinant oncolytic adenoviruses for 48 h (MOI=5) and then subjected to the EdU labeling according to the manufacturer's instructions for the EdU cell proliferation detection kit (Sangon Biotech, Shanghai, China).

Animal experiment. All animal protocols were approved by the Institutional Animal Handling and Use Committee

(Scheme No.: SIBCB-S581-1609-027-C1). The animal welfare and laboratory procedures were strictly carried out in accordance with the Guide to Laboratory Animal Regulations and Standards. The experiments were monitored once a day and terminated on humanitarian grounds. The mice were euthanized by carbon dioxide asphyxiation and then dissected, and all efforts were made to minimize suffering. Female BALB/c (4–5 weeks) were purchased from Shanghai Experimental Animal Center, Chinese Academy of Sciences (SLAC, Shanghai, China). These experiments were conducted in a specific pathogen-free (SPF) level laboratory, Shanghai Institute for Biological Sciences, Chinese Academy of Sciences. The HGC-27 cells (1×10^6) were injected subcutaneously into nude mice to establish the tumor xenograft model. When the tumors were 80–100 mm³, the nude mice were randomly divided into 5 groups with five mice in each group, plus 5 untreated nude mice, a total of 30 nude mice. The mice were injected with different recombinant oncolytic adenoviruses (1×10^8 PFU/mouse) or PBS every other day for three consecutive times. Tumor length and width were measured every other day after injection to calculate tumor volume: Volume = (Width² × Length)/2. All nude mice and data were included in the analysis. Finally, tumors were harvested for analysis, and the nick terminal labeling of dUTP biotin mediated by terminal deoxynucleotide transferase was performed.

TUNEL assay. The tumor tissues were fixed with 4% polymethanol for 6 h and subsequently dehydrated with 30% sucrose. The 6 μ m tissue sections were analyzed by using an apoptosis detection kit (red fluorescence, Cat #C1089, Beyotime, Shanghai, China). The procedure was carried out according to the manufacturer's instructions. The specimens were incubated with TUNEL at 37°C for 60 min and subjected to staining with 4',6-diamidino-2-phenylindole

(DAPI) at room temperature for 30 min. The specimens were sealed with anti-fluorescence quenching solution and observed under a fluorescence microscope.

Statistical analysis. The experiments were performed in triplicate and the values are presented as mean \pm SD. Student's t-test or one-way analysis of variance using was used for statistical analysis with the help of Prism GraphPad 8 software. * $p < 0.05$, ** $p < 0.01$, and *** $p < 0.001$ were taken as the measure the statistically significant differences.

Results

Construction and characterization of the oncolytic adenovirus. To identify the oncolytic adenovirus we had constructed, the corresponding PCR primers were designed and determined its location (Figure 1a). The target gene was identified by PCR, *mK5*-F primers and *mK5*-R primers were used to identify the *mK5* gene (Figure 1b, channel 4), *MnSOD*-F and *MnSOD*-R primers were used to identify the *MnSOD* gene (Figure 1b, channel 6), *Surp*-F and *Surp*-R primers were used to identify *Survivin* genes (Figure 1b, channel 2), wild-type primers wild-F and wild-R were used to identify wild-type oncolytic adenovirus (Figure 1b, channels 1, 3, and 5). The gel electrophoresis results showed that the structure of our recombinant oncolytic adenovirus was reasonable. The constructed oncolytic adenovirus was used to infect HGC-27 cells and the protein expression of *mK5* and *MnSOD* were examined by western blot (Figure 1c), which indicated that the constructed oncolytic adenoviruses could be expressed in gastric cancer cells.

Selective killing effect of recombinant oncolytic adenovirus on gastric cancer cells *in vitro*. To detect the killing effect of oncolytic adenovirus *in vitro*, we used Ad-Surp-empty, Ad-Surp-*mK5*, Ad-Surp-*MnSOD*, Ad-Surp-*mK5*, and Ad-Surp-*MnSOD* in combination with gradient MOI to infect GC cell lines HGC-27, NCI-87, AGS and human normal cells, human lung epithelial cell Beas-2B, human liver cell QSG-7701, human colon epithelial cell NCM-460, and CCK-8 assay was used to detect their cell viability for 4 consecutive days. The cell viability of cancer cells treated with various oncolytic adenoviruses decreased significantly (Figures 2a–2f), while the cell activity of all kinds of normal human cells did not decrease significantly. The survival rate of cells at 72 and 96 h was above 80%, indicating that the newly constructed oncolytic adenoviruses had certain selectivity in killing the cells (Figures 2g–2i). At the same time, the combination of Ad-Surp-*mK5*/*MnSOD* (Volume ratio = 1:1) had the strongest killing effect, and the one with significant effect was observed on HGC-27 cells. The proliferation of HGC-27 cells was analyzed by the EdU assay and the same result was obtained (Figure 3).

Apoptosis induced by recombinant oncolytic adenovirus in gastric cancer cells. Next, the recombinant oncolytic adenovirus-induced cell death through apoptosis was analyzed. We first detected the morphological changes

of apoptosis in HGC-27 and QSG-7701 using Hoechst method. The results of the Hoechst 33342 fluorescent staining showed that the apoptotic rate of HGC-27 cells was higher under Ad-Surp-*mK5*/*MnSOD* (1:1) combination as compared to Ad-Surp-*mK5* or Ad-Surp-*MnSOD* treatments alone (Figures 4a–4e), which was about twice as high as that treated with the virus alone (Figure 4k). QSG-7701 cells treated in the same way showed no significant difference in cell morphology compared with the control group (Figures 4f–4j), and the same situation was observed after statistical analysis (Figure 4k). The apoptotic characteristics were reduced cell volume, condensed nucleoplasm, degradation of the nucleus into fragments, and formation of apoptotic bodies. Similarly, a flow cytometry analyzer was used to detect the apoptosis of HGC-27 cells (Figure 4l). Ad-Surp-Empty, Ad-Surp-*mK5*, Ad-Surp-*MnSOD*, Ad-Surp-*mK5*/*MnSOD* (1:1) combined application was used to infect cells for 48 h (MOI = 5). The results showed that the apoptosis of cells in the newly constructed virus combined application group was significantly higher than that in the other groups, and the cell apoptosis rate of the newly constructed virus combined application group accounted for about 120% of the virus alone application group.

Western blot analysis was performed to detect the content of major apoptosis-related proteins in the two signaling pathways (mitochondrial-dependent apoptosis and independent apoptosis). As shown in Figure 5, oncolytic adenovirus activates the caspase-dependent apoptotic signaling pathway. The levels of Cleaved-caspase 3, Cleaved-caspase 8, and Cleaved-caspase 9 were increased in the Ad-Surp-*mK5*/*MnSOD* (1:1) combination group compared to the virus alone group and the PBS group, as were the levels of Bax, an apoptotic promoter protein. However, the contents of PARP and Bcl-2 were reduced. The effects of the Ad-Surp-*mK5*/*MnSOD* (1:1) combination on the apoptosis-related proteins were comparatively more significant than Ad-Surp-*mK5* or Ad-Surp-*MnSOD* treatments alone.

These results indicate that the Ad-Surp-*mK5*/*MnSOD* (1:1) combination activates the apoptosis signaling pathway in gastric cancer cells more than the other treatment groups and eventually promotes cell apoptosis.

Antitumor effect of a newly constructed oncolytic adenovirus Ad-Surp-*mK5*/*MnSOD* combination *in vivo*. To verify the antitumor activity of the newly constructed oncolytic adenovirus against gastric cancer in nude mice, we established a mouse model of gastric cancer xenotransplantation. The tumor measurement method, drug administration method, and final treatment effect on the mice are shown in Figures 6a and 6b. Compared to the recombinant oncolytic adenovirus alone treatment group and the PBS group, the anti-tumor effect of the Ad-Surp-*mK5*/*MnSOD* combination group was significantly enhanced. Additionally, a similar therapeutic effect was observed on the tumor growth (Figure 6c), showing that the tumor volume in the Ad-Surp-*mK5*/*MnSOD* combination group decreased by 70% compared to

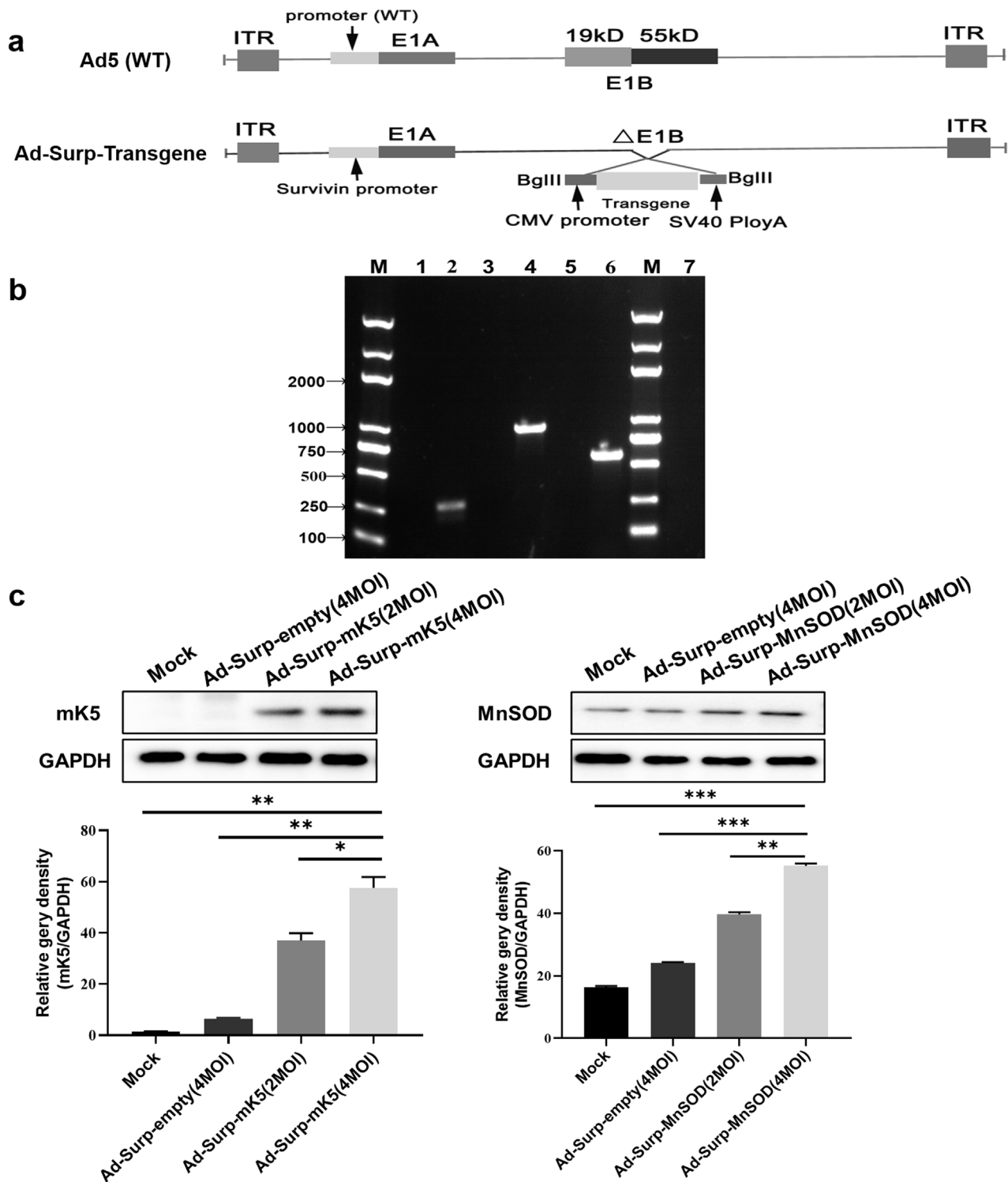


Figure 1. Construction and identification of Ad-Surp-Transgene. a) Transgene includes mutants of mK5, MnSOD with wild-type adenovirus Ad5 as a skeleton, mK5: human plasminogen Kringle 5; MnSOD: manganese superoxide dismutase. b) Correlative identification of three kinds of recombinant oncolytic adenovirus Ad-Surp-empty, Ad-Surp-MnSOD, and Ad-Surp-mK5. Channels 7 were negative control, and channels 1, 3, and 5 were wild virus identification. The survivin, MnSOD, and mK5 genes were identified in channels 2, 4, and 6. c) Western blot analysis showed the protein expression level of mK5 or MnSOD in HGC-27 cells treated with Ad-Surp-empty, Ad-Surp-mK5, or Ad-Surp-MnSOD, PBS for 48 h. The data are shown as the mean \pm SD of three independent experiments. * $p < 0.05$, ** $p < 0.01$, *** $p < 0.001$

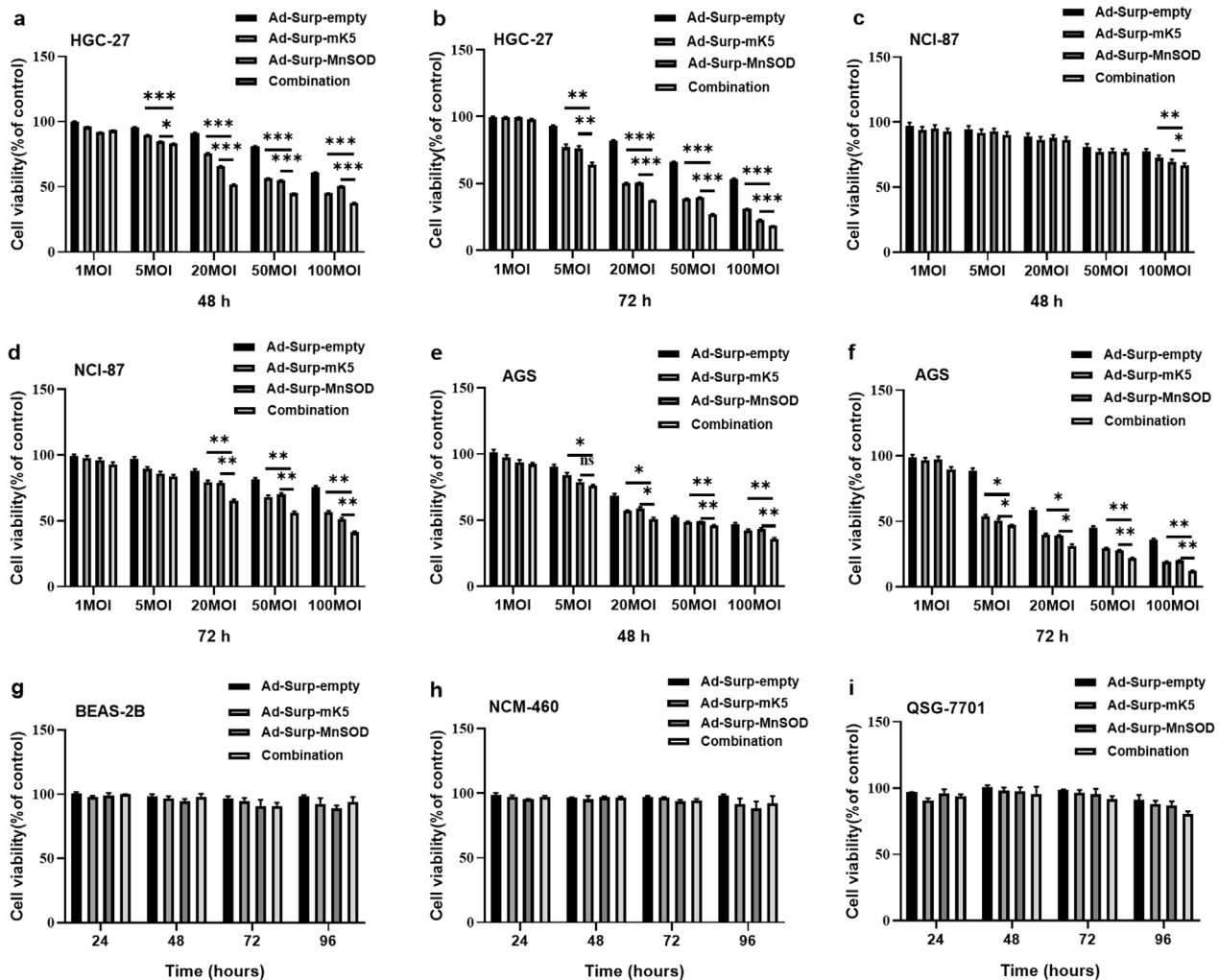


Figure 2. Selective killing effect of recombinant oncolytic adenovirus on gastric cancer. CCK-8 assay was used to analyze the cell activity of Ad-Surp-Empty, Ad-Surp-mK5, Ad-Surp-MnSOD, Ad-SurpmK5, and Ad-Surp-MnSOD combined treatment on HGC-27 infected with different viruses for 48 h (a) and 72 h (b). The cell viability of NCI-87 for 48 h (c), and 72 h (d), AGS for 48 h (e) and 72 h (f) were similarly observed. CCK-8 assay was used to detect the recombinant oncolytic adenovirus alone, Ad-Surp-mK5 and Ad-Surp-MnSOD (1:1) combined use had no statistical significance on the cell viability of normal human cells Beas-2B (g), NCM-460 (h), and QSG-7701 (i) at 24, 48, 72, and 96 h when MOI was 20. The data are shown as mean \pm SD of three independent experiments. * $p < 0.05$, ** $p < 0.01$, *** $p < 0.001$

the PBS group, and the efficacy was almost double that of the Ad-Surp-mK5 or Ad-Surp-MnSOD alone groups. The body weight of the experimental mice was measured during the experiment (Figure 6d), there was no significant difference in body weight between the experimental mice in each group and the normal tumor-free nude mice. After tumor resection, the body weight and tumor mass of mice in each group were compared respectively (Figures 6e, 6f). There was no significant difference in the body weight of each experimental mouse. However, in the tumor mass analysis of each group, the tumor mass of the virus combination group was significantly lower than those of the other treatment groups. When cells enter apoptosis, DNA ladders are generated by activation of some endonuclease, the exposed 3'-OH is

labeled by dUTP catalyzed by terminal deoxynucleic acid transferase (TdT). To further verify the apoptotic status of oncolytic adenovirus-infected tumors, the tissue immunofluorescence test was performed (Figures 7a, 7b). The results showed that the Ad-Surp-mK5/MnSOD combination treatment group significantly inhibited the tumor growth and induced a higher level of apoptosis as compared to other groups. No adverse events occurred during the experiment.

Discussion

The present study employed a strategy called CTGVT [31], to design a dual-regulatory oncolytic adenovirus vector, Ad-Surp-E1A- Δ E1B, that can replicate normally

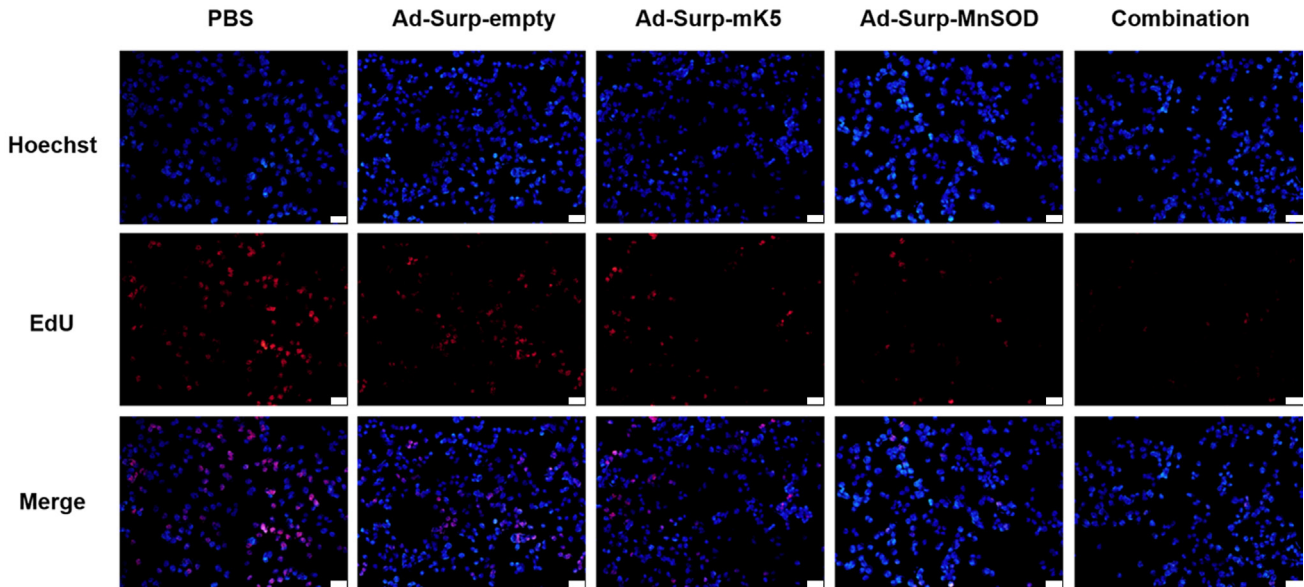


Figure 3. EdU cell proliferation detection. The cell proliferation of Ad-Surp-empty, Ad-Surp-*mK5*, Ad-Surp-*MnSOD*, Ad-Surp-*MnSOD*, and Ad-Surp-*mK5* (1:1) combination infected with HGC-27 48 h was observed under fluorescence microscope (MOI=5, Blue fluorescence, Hoechst 33342 staining; Red fluorescence, Apollo staining, scale bar=50 μ m). The data are shown as mean \pm SD of three independent experiments. * p <0.05, ** p <0.01, *** p <0.001

and cause tumor cell lysis in survivin-positive GC cells that lack P53 function [32]. Our results indicate that mutant *K5* and a tumor suppressor gene *MnSOD* can inhibit tumor growth by inducing tumor cell apoptosis. Ad-Surp-*mK5* in combination with Ad-Surp-*MnSOD* (Volume ratio = 1:1) can significantly inhibit the tumor growth in HGC-27 xenograft tumors, and the inhibition effect is more severe than that of the other two recombinant oncolytic adenoviruses alone. These findings suggest that the combined use of Ad-Surp-*mK5* and Ad-Surp-*MnSOD* has great potential in the treatment of GC. Li et al. showed that *mK5* can induce apoptosis of endothelial cells both *in vivo* and *in vitro*, and is a more effective anti-angiogenic drug than *K5* [13]. At the same time, in mature endothelial cells, ROS are an important mediator of different signaling pathways related to angiogenesis and cell metabolism, regulation of cell proliferation, migration, and gene expression [33]. Hypoxia-induced vascular endothelial growth factor (VEGF) expression plays a key role in the promotion of tumor angiogenesis. At present, the molecular mechanism of its regulation under hypoxic conditions has been studied. Xu et al. found that induction of VEGF in hypoxic HepG2 cells was ROS-dependent [34]. Studies have shown that ROS-mediated signals play a key role in the regulation of transcription during hypoxia, and it has been reported that ROS-dependent mechanisms induce VEGF to enter cancer cells under hypoxia conditions. Existing ROS scavengers can reduce the expression of VEGF [35], while *MnSOD* is the main antioxidant in mitochondria, which can resist ROS

by catalyzing the transformation of ROS from superoxide anion (O_2^-) to hydrogen peroxide (H_2O_2) in mitochondria [36]. The deletion of *MnSOD* in various tumors suggests that *MnSOD* may be a tumor suppressor gene.

In the present study, we constructed two novel survivin-regulated, dual-targeted oncolytic adenovirus Ad-Surp-*mK5/MnSOD*, which carries the gene *mK5* or *MnSOD*. Our current data revealed that the anti-tumor efficacy of Ad-Surp-*mK5* and Ad-Surp-*MnSOD* (1:1) combination in the treatment of gastric cancer is significantly better than that of Ad-Surp-*mK5* and Ad-Surp-*MnSOD* alone. It was further demonstrated that compared to the recombinant adenovirus alone, the combination of the virus induced apoptosis of gastric cancer cells specifically, and the expression of caspase cleaved was stronger. Additionally, no toxicity was found in human lung epithelial cells, human liver cells, and human colon cells *in vitro* as revealed by the CCK-8 assay. The above data show that our new construct is a potential candidate for experimental GC anticancer drug. Using CTGVT strategy to ensure the safety of viral vector, we put the virus E1B knockout Ad5 as the initial viral vector, but simply deleted the viral gene does not stop unnecessary tissue damage, tumor selectivity can be enhanced by the placement of a tumor-specific promoter that is transcribed via mRNA upstream of a critical viral gene (E1A), so we used a tumor-specific *Survivin* promoter [37]. *Survivin* promoter regulation of the E1A gene makes up for the lack of selectivity of the OV vector. Adenovirus with anti-cancer therapy gene after recombination proliferates and

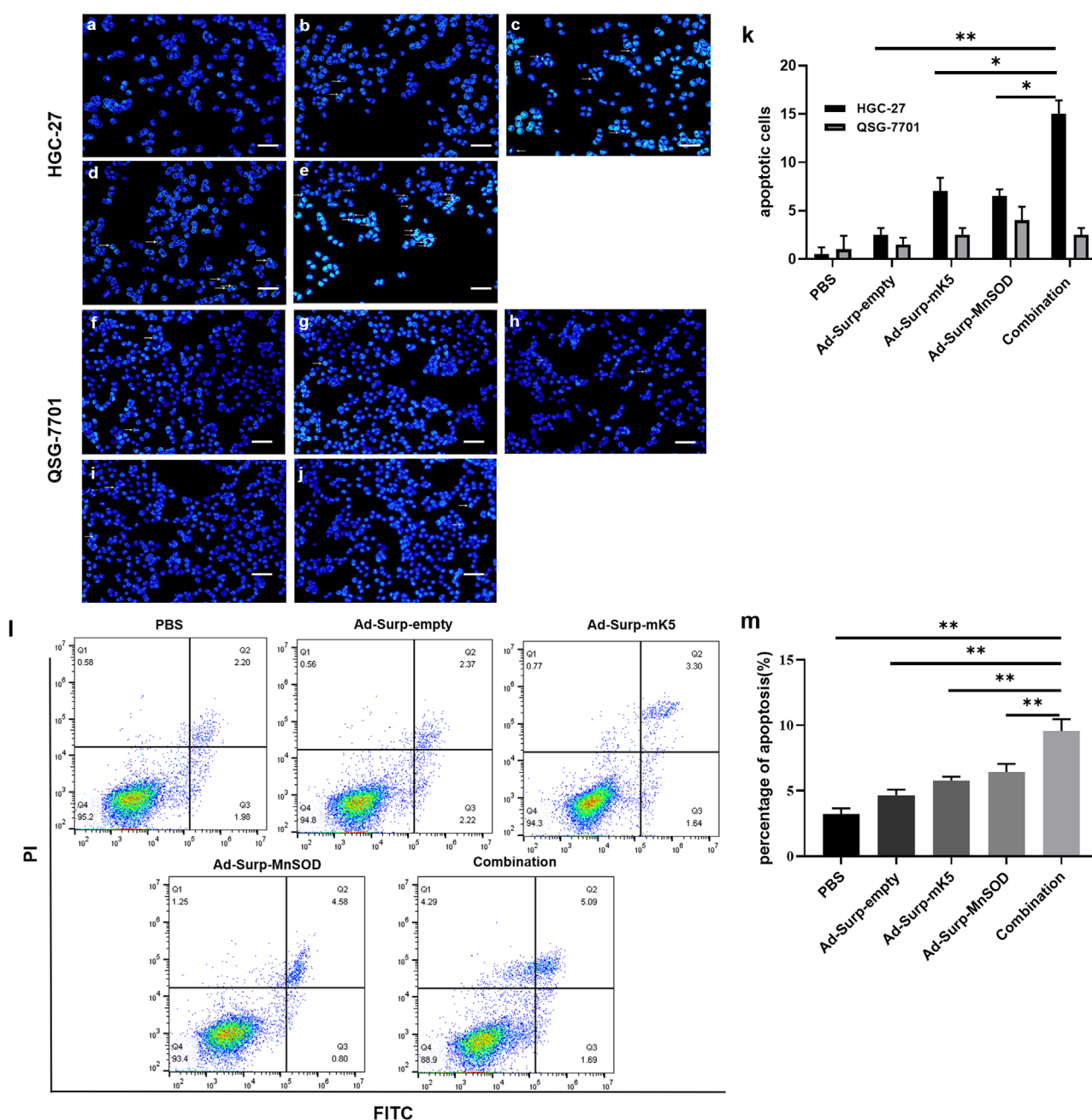


Figure 4. Various recombinant oncolytic adenoviruses selectively induce apoptosis and the mechanism of action. HGC-27 (A–E) and QSG-7701 (F–J) were infected with phosphate (PBS) (a, f), Ad-Surpempty (b, g), Ad-Surp-mK5 (c, h), Ad-Surp-MnSOD (d, i), Ad-Surp-mK5 and Ad-Surp-MnSOD combination (1:1) (e, j) for 48 h (MOI = 5), cell apoptosis was detected by Hoechst 33342 staining. Chromatin karyokinization (indicated by arrow) was observed under a fluorescence microscope, scale bar = 20 μ m. (k) In Figures a–j, HGC-27 and QSG-7701 cells are stained by Hoechst 33342, and the number of apoptotic cells is observed under fluorescence microscopy. (l–m) HGC-27 cells were treated with different recombinant oncolytic adenovirus 48 h, and the PBS treatment group was the control group (MOI = 5). The data are shown as mean \pm SD of three independent experiments. * $p < 0.05$, ** $p < 0.01$, *** $p < 0.001$

replicates in gastric cancer cells, triggering the release of progeny virus and which subsequently infect and eventually destroy and kill the cancer cells. Chen et al. reported that when a system-managed suicide gene is driven by a *Survivin* promoter, systemic toxicity may be significantly reduced

[38]. Meanwhile, *Survivin* promoters have been shown to induce transgenic overexpression in cancer [11].

Oncolytic therapy is another form of immune stimulation that works through the patient's own immune system to combat tumor growth and facilitate tumor removal [39].

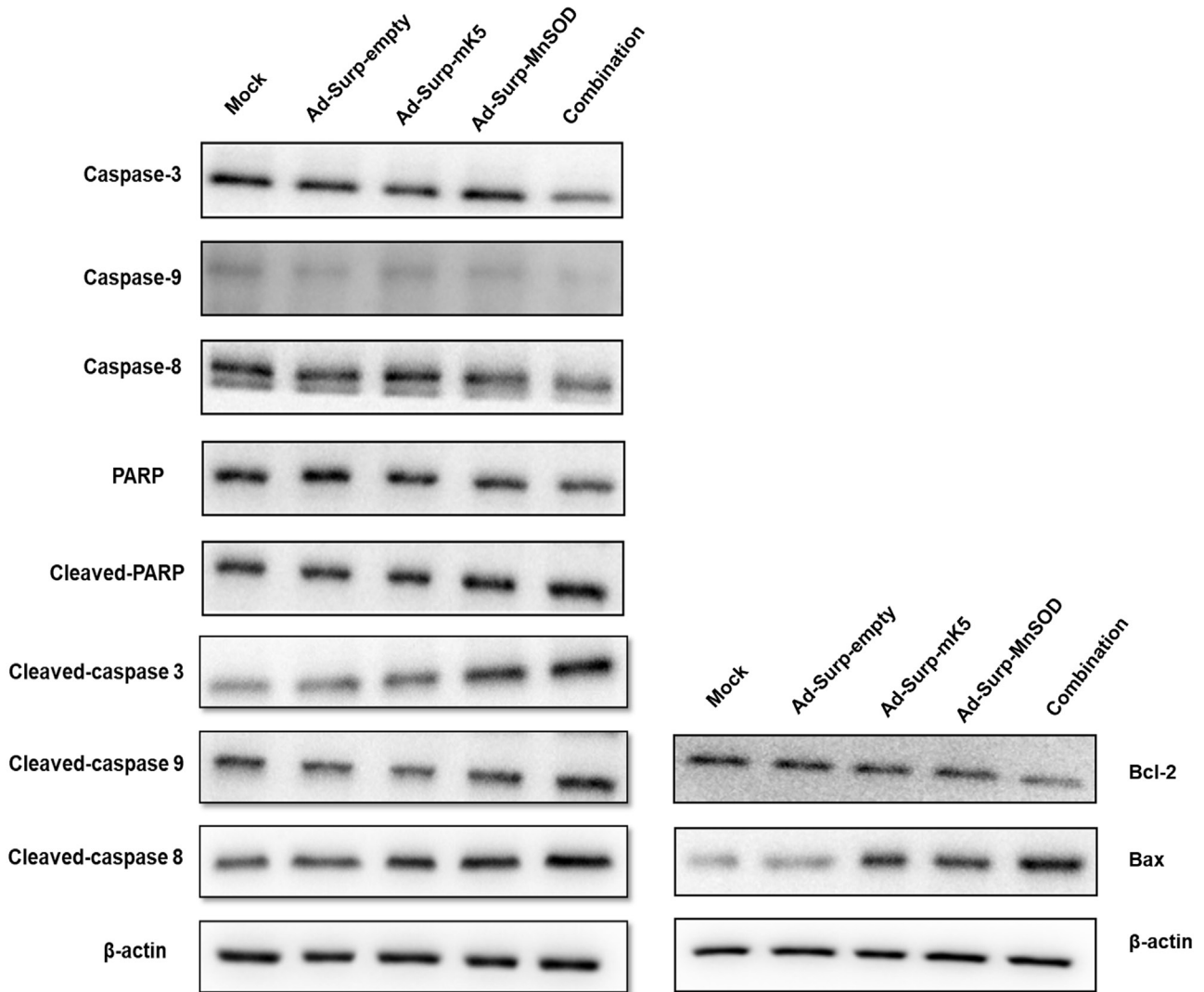


Figure 5. Detection of protein expressions associated with virus proliferation and apoptosis by western blot. As described above, expression of caspase-3, caspase-9, caspase-8, PARP, Cleaved-PARP, Cleaved-caspase 3, Cleaved-caspase 9, Cleaved-caspase 8, apoptotic proteins Bcl-2, and Bax was observed after treatment of HGC-27 cells by different viruses.

In this study, the generation of immunogenicity was largely avoided by intratumoral injection. Although our novel survivin-regulated, dual-targeted OVs have achieved powerful antitumor effects in GC cells and animal models, there are still some challenges that need to be further addressed. The antiproliferative effects of Ad-Surp-*mK5/MnSOD* against the GC cells still remain low. Although they carry therapeutic genes *mK5* or/and *MnSOD* and soluble tumor recombinant adenoviruses effectively inhibit the growth of nude mice tumors, they can't completely eradicate tumor xenograft. The primary reason for this result may be the host immune response and the limited distribution of the OVs in the tumor tissues [40]. The type and size capsule of viruses and the nature of the tumor microenvironment affect the penetration and diffu-

sion of the OVs [41], and the size of the insert fragment is limited. Therefore, it is urgent to address such problems in future virus-gene targeted cancer therapy and to achieve more significant therapeutic effects through the combination of other conventional therapies, whether survivin inhibitors affect the effect of combined genes. In addition, how to avoid the impact will require further research.

In conclusion, OV successfully constructed by CTGVT strategies, through the *Survivin* promoter regulation targeting tumor adenovirus vector which makes the recombinant adenovirus in GC cells more specific. It can effectively mediate the *mK5* or *MnSOD* gene expression maximizing the role of dissolving the tumor and inhibiting the tumor growth while minimizing side effects on normal tissues. However,

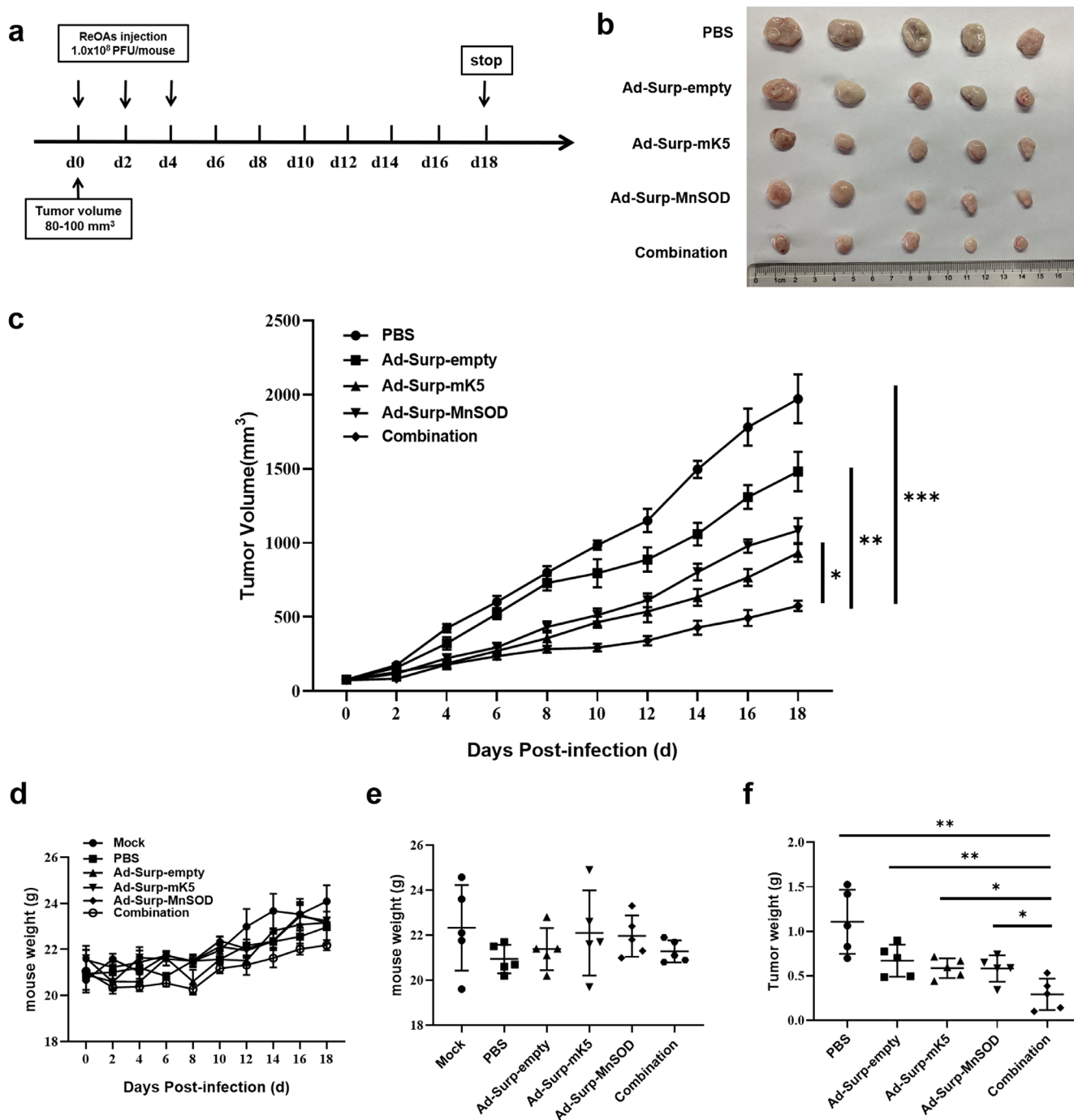


Figure 6. *In vivo* antitumor effect of recombinant oncolytic adenovirus. HGC-27 cells (1×10^6) were subcutaneously injected into female BALB/c nude mice to establish a mouse tumor xenograft model. a) When the tumor grew to 80–100 mm³, the nude mice were randomly divided into 5 groups (n=5). The mice were injected with different recombinant oncolytic adenovirus (ReOAs) 1.0×10^8 PFU/mouse every other day for 3 consecutive intratumor injections. Tumor volume was measured with a vernier caliper every other day, and the experiment was stopped on the 18th day. b) Photographs of anatomical tumors of nude mice treated with different adenoviruses. c) Tumor growth trend of mice Tumor: Volume (mm³) = (Length \times Width²)/2. d) Changes in body weight of mice in each group during the experiment showed no statistical significance among each group. e) The final body weight of nude mice was measured by tumor resection after the end of the experiment, and there was no statistical significance among all groups. f) The final mass of tumors in each group at the end of the experiment. The data are shown as mean \pm SD of three independent experiments. * $p < 0.05$, ** $p < 0.01$, *** $p < 0.001$

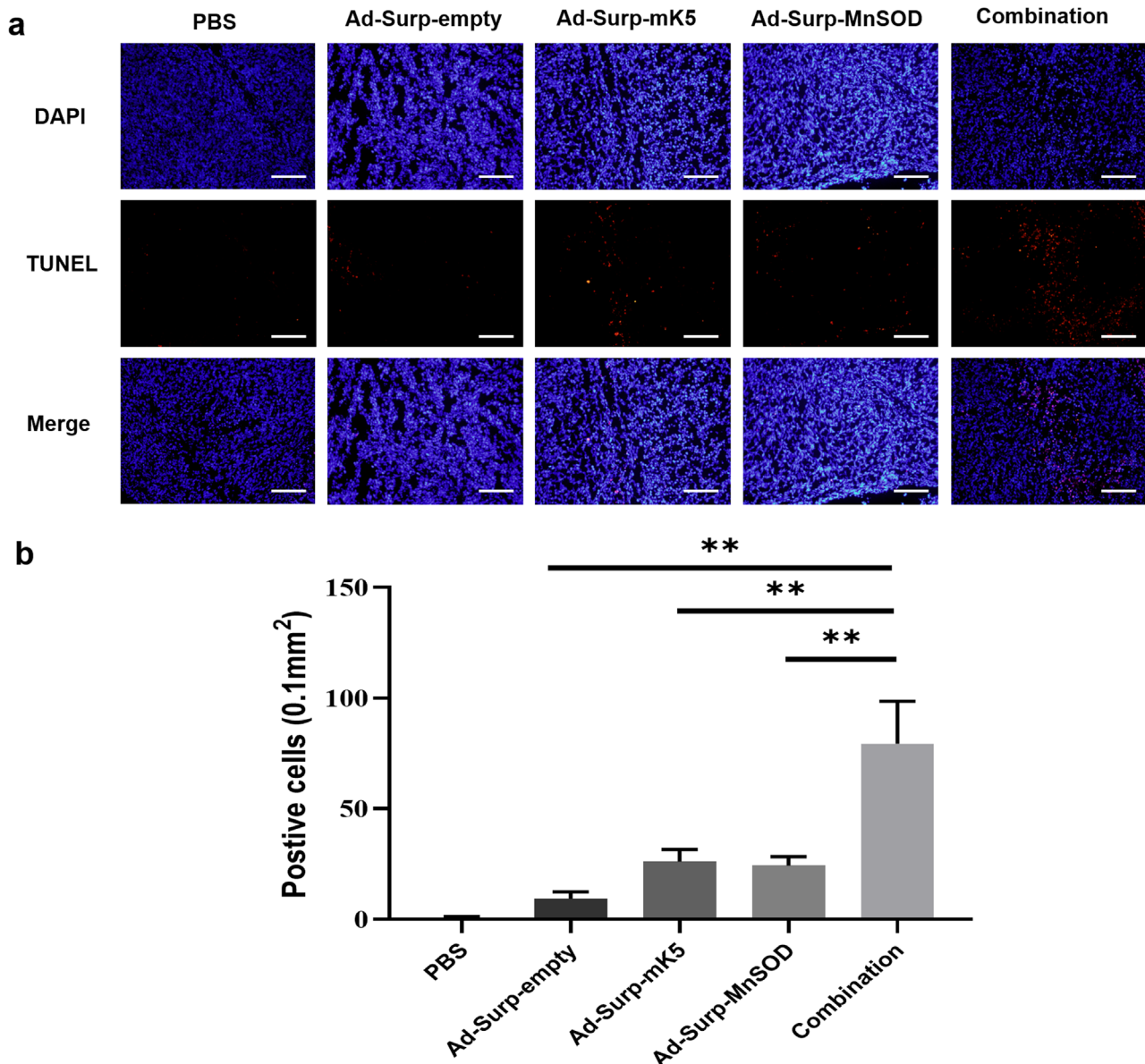


Figure 7. Detection of apoptosis rate of tissue cells by TUNEL staining. a) Tumor fixation, embedding, and cryopreservation were performed after tumor dissection in nude mice, and the thickness of frozen tissue sections was 6 μm (Blue fluorescence, DAPI staining; Red fluorescence, TUNEL positive staining), scale bar = 200 μm . b) Statistical analysis of positive cells detected by TUNEL staining. The data are shown as mean \pm SD of three independent experiments. * $p < 0.05$, ** $p < 0.01$, *** $p < 0.001$

this study also has some limitations. Due to the limitations of time and funds, we did not establish the tumor model in situ, which may lead to errors in the actual therapeutic effect, and the study on the mechanism is not in-depth enough. Therefore, further research on its mechanism is needed in the future.

Generally, the combined therapy of *mK5* and *MnSOD* recombinant oncolytic adenovirus has a wider application prospect and may prove to be an important candidate for the treatment of GC.

Acknowledgments: The authors would like to thank the staff of the Shanghai Institute for Biological Sciences and our colleagues for their support of this study.

References

- [1] SMYTH EC, NILSSON M, GRABSCH HI, VAN GRIEKEN NCT, LORDICK F. gastric cancer. *The Lancet* 2020; 396: 635–648. [https://doi.org/10.1016/S0140-6736\(20\)31288-5](https://doi.org/10.1016/S0140-6736(20)31288-5)

- [2] SONG Z, WU Y, YANG J, YANG D, FANG X. Progress in the treatment of advanced gastric cancer. *Tumour Biol* 2017; 39: 1010428317714626. <https://doi.org/10.1177/1010428317714626>
- [3] TAN Z. Recent advances in the surgical treatment of advanced gastric cancer: a review. *Med Sci Monit* 2019; 25: 3537–3541. <https://doi.org/10.12659/MSM.916475>
- [4] SMYTH EC, MOEHLER M. Late-line treatment in metastatic gastric cancer: today and tomorrow. *Ther Adv Med Oncol* 2019; 11: 1758835919867522. <https://doi.org/10.1177/1758835919867522>
- [5] SURGERY NGRUG. Quality and outcomes in global cancer surgery: protocol for a multicentre, international, prospective cohort study (GlobalSurg 3). *BMJ Open* 2019; 9: e026646. <https://doi.org/10.1136/bmjopen-2018-026646>
- [6] FUKUHARA H, INO Y, TODO T. Oncolytic virus therapy: a new era of cancer treatment at dawn. *Cancer Sci* 2016; 107: 1373–1379. <https://doi.org/10.1111/cas.13027>
- [7] ZHENG M, HUANG J, TONG A, YANG H. Oncolytic viruses for cancer therapy: barriers and recent advances. *Mol Ther Oncolytics* 2019; 15: 234–247. <https://doi.org/10.1016/j.omto.2019.10.007>
- [8] GORADEL NH, MOHAJEL N, MALEKSHAHI ZV, JAH-ANGIRI S, NAJAFI M et al. Oncolytic adenovirus: a tool for cancer therapy in combination with other therapeutic approaches. *J Cell Physiol* 2019; 234: 8636–8646. <https://doi.org/10.1002/jcp.27850>
- [9] ABUDOUREYIMU M, LAI Y, TIAN C, WANG T, WANG R et al. Oncolytic adenovirus—a nova for gene-targeted oncolytic viral therapy in HCC. *Front Oncol* 2019; 9: 1182. <https://doi.org/10.3389/fonc.2019.01182>
- [10] LIN KY, CHENG SM, TSAI SL, TSAI JY, LIN CH et al. Delivery of a survivin promoter-driven antisense survivin-expressing plasmid DNA as a cancer therapeutic: a proof-of-concept study. *Onco Targets Ther* 2016; 9: 2601–2613. <https://doi.org/10.2147/OTT.S101209>
- [11] CHEN JS, LIU JC, SHEN L, RAU KM, KUO HP et al. Cancer-specific activation of the survivin promoter and its potential use in gene therapy. *Cancer Gene Ther* 2004; 11(1): 740–747. <https://doi.org/10.1038/sj.cgt.7700752>
- [12] CHANG Y, MOCHALKIN I, MCCANCER SG, CHENG B, TULINSKY A et al. Structure and ligand binding determinants of the recombinant kringle 5 domain of human plasminogen. *Biochemistry* 1998; 37: 3258–3271. <https://doi.org/10.1021/bi972284e>
- [13] LI C, LI L, CHENG R, DAI Z, LI C et al. Acidic/neutral amino acid residues substitution in NH₂ terminal of plasminogen kringle 5 exerts enhanced effects on corneal neovascularization. *Cornea* 2013; 32: 680–688. <https://doi.org/10.1097/ICO.0b013e3182781ec9>
- [14] FAN JK, XIAO T, GU JF, WEI N, HE LF et al. Increased suppression of oncolytic adenovirus carrying mutant k5 on colorectal tumor. *Biochem Biophys Res Commun* 2008; 374: 198–203. <https://doi.org/10.1016/j.bbrc.2008.07.005>
- [15] HAO J, XIE W, LI H, LI R. Prostate Cancer-Specific of DD3-driven Oncolytic Virus-harboring mK5 Gene. *Open Med (Wars)* 2019; 14: 1–9. <https://doi.org/10.1515/med-2019-0001>
- [16] BORRELLI A, SCHIATTARELLA A, BONELLI P, TUC-CILLO FM, BUONAGURO FM et al. The functional role of MnSOD as a biomarker of human diseases and therapeutic potential of a new isoform of a human recombinant MnSOD. *Biomed Res Int* 2014; 2014: 476789. <https://doi.org/10.1155/2014/476789>
- [17] SUN G, WANG Y, HU W, LI C. Effects of manganese superoxide dismutase (MnSOD) expression on regulation of esophageal cancer cell growth and apoptosis in vitro and in nude mice. *Tumour Biol* 2013; 34: 1409–1419. <https://doi.org/10.1007/s13277-012-0622-x>
- [18] ZHANG Y, SMITH BJ, OBERLEY LW. Enzymatic activity is necessary for the tumor-suppressive effects of MnSOD. *Antioxid Redox Signal* 2006. <https://doi.org/10.1089/ars.2006.8.1283>
- [19] FAN JJ, HSU WH, HUNG HH, ZHANG WJ, LEE YA et al. Reduction in MnSOD promotes the migration and invasion of squamous carcinoma cells. *Int J Oncol* 2019; 54: 1639–1650. <https://doi.org/10.3892/ijo.2019.4750>
- [20] LI X, SHEN M, CAI H, LIU K, LIU Y et al. Association between manganese superoxide dismutase (MnSOD) polymorphism and prostate cancer susceptibility: a metaanalysis. *Int J Biol Markers* 2016; 31: e422–e430. <https://doi.org/10.5301/ijbm.5000188>
- [21] SARSOOR EH, KALEN AL, GOSWAMI PC. Manganese superoxide dismutase regulates a redox cycle within the cell cycle. *Antioxid Redox Signal* 2014; 20: 1618–1627. <https://doi.org/10.1089/ars.2013.5303>
- [22] TORRENS-MAS M, CORDANI M, MULLAPPILLY N, PACCHIANA R, RIGANTI C et al. Mutant p53 induces SIRT3/MnSOD axis to moderate ROS production in melanoma cells. *Arch Biochem Biophys* 2020; 679: 108219. <https://doi.org/10.1016/j.abb.2019.108219>
- [23] SUN W, WANG B, QU XL, ZHENG BQ, HUANG WD et al. Metabolism of reactive oxygen species in osteosarcoma and potential treatment applications. *Cells* 2019; 9: 87. <https://doi.org/10.3390/cells9010087>
- [24] BONETT R. Potential therapeutic applications of MnSODs and SOD-mimetics. *Chemistry* 2018; 24: 5032–5041. <https://doi.org/10.1002/chem.201704561>
- [25] WANG S, SHU J, CHEN L, CHEN X, ZHAO J et al. Synergistic suppression effect on tumor growth of ovarian cancer by combining cisplatin with a manganese superoxide dismutase-armed oncolytic adenovirus. *Onco Targets Ther* 2016; 9: 6381–6388. <https://doi.org/10.2147/OTT.S113014>
- [26] ISNAINI I, PERMATASARI N, MINTAROEM K, PRIHARDINA B, WIDODO MA. Oxidants-Antioxidants Profile in the breast cancer cell line MCF-7. *Asian Pac J Cancer Prev* 2018; 19: 3175–3178. <https://doi.org/10.31557/APJCP.2018.19.11.3175>
- [27] NALKIRAN I, TURAN S, ARIKAN S, KAHRAMAN OT, ACAR L et al. Determination of gene expression and serum levels of MnSOD and GPX1 in colorectal cancer. *Anticancer Res* 2015; 35: 255–259.
- [28] LI G, LI X, WU H, YANG X, ZHANG Y et al. CD123 targeting oncolytic adenoviruses suppress acute myeloid leukemia cell proliferation in vitro and in vivo. *Blood Cancer J* 2014; 4: e194. <https://doi.org/10.1038/bcj.2014.15>

- [29] KONZACK A, JAKUPOVIC M, KUBAICHUK K, GORLACH A, DOMBROWSKI F et al. Mitochondrial dysfunction due to lack of manganese superoxide dismutase promotes hepato-carcinogenesis. *Antioxid Redox Signal* 2015; 23: 1059–1075. <https://doi.org/10.1089/ars.2015.6318>
- [30] OUGH M, LEWIS A, ZHANG Y, HINKHOUSE MM, RITCHIE JM et al. Inhibition of cell growth by overexpression of manganese superoxide dismutase (MnSOD) in human pancreatic carcinoma. *Free Radic Res* 2004; 38: 1223–1233. <https://doi.org/10.1080/10715760400017376>
- [31] LIU XY. Targeting gene-virotherapy of cancer and its prosperity. *Cell Res* 2006; 16: 879–886. <https://doi.org/10.1038/sj.cr.7310108>
- [32] KIRN DH, MCCORMICK F. Replicating viruses as selective cancer therapeutics. *Molecular Medicine Today* 1996; 2: 519–527. [https://doi.org/10.1016/s1357-4310\(97\)81456-6](https://doi.org/10.1016/s1357-4310(97)81456-6)
- [33] YANG Z, VON BALLMOOS MW, FAESSLER D, VOELZMANN J, ORTMANN J et al. Paracrine factors secreted by endothelial progenitor cells prevent oxidative stress-induced apoptosis of mature endothelial cells. *Atherosclerosis* 2010; 211: 103–109. <https://doi.org/10.1016/j.atherosclerosis.2010.02.022>
- [34] HU Z, DONG N, LU D, JIANG X, XU J et al. A positive feedback loop between ROS and Mxi1-0 promotes hypoxia-induced VEGF expression in human hepatocellular carcinoma cells. *Cell Signal* 2017; 31: 79–86. <https://doi.org/10.1016/j.cellsig.2017.01.007>
- [35] KIM YM, KIM SJ, TATSUNAMI R, YAMAMURA H, FUKAITI et al. ROS-induced ROS release orchestrated by Nox4, Nox2, and mitochondria in VEGF signaling and angiogenesis. *Am J Physiol Cell Physiol* 2017; 312: C749–C764. <https://doi.org/10.1152/ajpcell.00346.2016>
- [36] KONZACK A, KIETZMANN T. Manganese superoxide dismutase in carcinogenesis: friend or foe? *Biochem Soc Trans* 2014; 42: 1012–1016. <https://doi.org/10.1042/BST20140076>
- [37] HAMID O, HOFFNER B, GASAL E, HONG J, CARVAJAL RD. Oncolytic immunotherapy: unlocking the potential of viruses to help target cancer. *Cancer Immunol Immunother* 2017; 66: 1249–1264. <https://doi.org/10.1007/s00262-017-2025-8>
- [38] LIU C, SUN B, AN N, TAN W, CAO L et al. Inhibitory effect of survivin promoter-regulated oncolytic adenovirus carrying P53 gene against gallbladder cancer. *Mol Oncol* 2011; 5: 545–554. <https://doi.org/10.1016/j.molonc.2011.10.001>
- [39] MARTIN NT, BELL JC. Oncolytic virus combination therapy: killing one bird with two stones. *Mol Ther* 2018; 26: 1414–1422. <https://doi.org/10.1016/j.ymthe.2018.04.001>
- [40] LAWLER SE, SPERANZA MC, CHO CF, CHIOCCA EA. Oncolytic viruses in cancer treatment: a review. *JAMA Oncol* 2017; 3: 841–849. <https://doi.org/10.1001/jamaoncol.2016.2064>
- [41] TAUBE JM, GALON J, SHOLL LM, RODIG SJ, COTTRELL TR et al. Implications of the tumor immune microenvironment for staging and therapeutics. *Mod Pathol* 2018; 31: 214–234. <https://doi.org/10.1038/modpathol.2017.156>